POLITECNICO DI TORINO
Repository ISTITUZIONALE

A practical method for gas changing time estimation using a simple gas-liquid mass transfer model

Original
A practical method for gas changing time estimation using a simple gas-liquid mass transfer model / Tarraran, L.; Lueckel, F. B.; Tommasi, T.; Contador, F. I. S.; Fino, D.. - In: JOURNAL OF MICROBIOLOGICAL METHODS. - ISSN 0167-7012. - 200:(2022). [10.1016/j.mimet.2022.106544]

Availability:
This version is available at: 11583/2981636 since: 2023-09-05T09:14:15Z

Publisher:
ELSEVIER

Published
DOI:10.1016/j.mimet.2022.106544

Terms of use:

This article is made available under terms and conditions as specified in the corresponding bibliographic description in the repository

Publisher copyright
Elsevier postprint/Author's Accepted Manuscript

© 2022. This manuscript version is made available under the CC-BY-NC-ND 4.0 license
http://creativecommons.org/licenses/by-nc-nd/4.0/.The final authenticated version is available online at:
http://dx.doi.org/10.1016/j.mimet.2022.106544

(Article begins on next page)

15 August 2024

A Practical Method for Gas Changing Time Estimation Using a Simple Gas-Liquid Mass Transfer Model

Loredana Tarraran [a*], Fabio Bozzolo Lueckel [b*], Tonia Tommasi [a], Felipe Ignacio Scott Contador [c], Debora Fino [a]

[a] Department of Applied Science and Technology, Politecnico di Torino, Corso Duca degli Abruzzi 24, Torino, 10129, Italy.

[b] Escuela de Ingeniería Bioquimica, Pontificia Universidad Católica de Valparaíso, Avenida Brasil 2147, Valparaíso, Chile.

[c] Green Technology Research Group, Facultad de Ingeniería y Ciencias Aplicadas, Universidad de los Andes, Monseñor Álvaro del Portillo 12455, Santiago, Chile.

* These authors equally contributed to this work.

Formatted: Not Highlight

Abstract

The present work explains a practical and simple method to calculate the gas changing time of anaerobic systems. It is substantiated under the physics of gas-liquid transfer theory and allows researchers to obtain an approximate value of gas changing time with few measurements of the gas composition in the outlet of the reactor. The only analytical equipment required is a gas analyzer, and calculations can be done using a spreadsheet. Along with the validation of the model, a short guide for its application in the laboratory is introduced. The model fit the experimental data with less than 1% error in the composition of the out-gas when no carbon dioxide is involved. This method will allow savings in

valuable resources such as time and gases while providing greater comprehension of the characteristics of the gas-liquid transfer of the studied system.

Keywords

Anaerobic fermentation; gas changing time; oxygen purging.

1. Introduction

Nowadays, the industry and research on bulk chemicals and third-generation biofuels based on carbon gases are growing because of the rising sensibility and higher regulations about decreasing greenhouse gas emissions. In particular, one of the more attractive carbon feedstocks is CO_2 due to its large availability and contribution to climate change. Several different agents, such as chemical catalysts, enzymes, and microorganisms can convert it into added-value compounds of industrial interest (Chauvy et al., 2019; Saravanan et al., 2021; Shi et al., 2015). According to the catalyst's nature, many CO_2 valorization processes occur in a liquid phase (usually water). The constant development of these technologies led to the establishment of different technologies to measure a specific gas (especially O_2 and CO_2) in the liquid phase.

In the case of CO_2 valorization employing anaerobic bacteria, the lack of oxygen and supply of feedstock is required. Nevertheless, these needs are often performed in two steps before inoculation for technical, environmental, and economic reasons. The first step is sparging the liquid phase with nitrogen to purge oxygen, and then the second is providing the gaseous feedstock.

In the literature, many protocols used nowadays involve a preparation step before starting the fermentation with anaerobic microorganisms, but these are described with huge variability between each other. To cite some examples, Maddipati and coworkers (2011) purged 3 L of culture medium (7.5 L total volume reactor) from oxygen using 12 L/h of N_2 for 24 hours. Then, syngas was piped in the fermenter at 9 L/h (for a not-reported period) before inoculation. Hoffmeister et al. (2016) purged 0.850 L of liquid culture medium (reactor of 2 L total volume), sparging N_2 for at least 12 h (in-flow gas rate was not reported). After this step, feeding gas was provided at 30 L/h for 1 h. In Al Rowaihi and coworkers (2018) study, a 1.6 L reactor was purged with 10 volumes of argon to remove any traces of oxygen from the medium, followed by 10 purges with the feeding gas mixture. Other studies (Kantzow and Weuster-Botz, 2016; Straub et al., 2014) describe a protocol in which 1 L of culture medium, in a reactor of 2 L total volume, was sparged with the feeding gas mixture for at least 12 h before inoculation of microorganism (in-flow gas rate was not reported). As suggested from the abovementioned examples, this preliminary step for setting up an anaerobic fermentation is time and resources consuming. Minimizing it would allow more sustainable processes concerning the environmental and economic point of view and optimize human efforts and employment of instruments. Nevertheless, some technical constraints often arise in experimental and pilot plants regarding monitoring the dissolved oxygen concentration and gaseous substrates saturation. Indeed, reactors could be designed without probes for dissolved gases to reduce capital costs. Moreover, the development of protocols might require dissolving gases different from those detected by the provided probes.

Gas solubilization in a liquid phase is explained by the gas-liquid mass transfer laws, which describe the concentration gradientof a certain gas between phases. In Figure 1 the difference in concentration through the interphase is shown. There are three major stages of transfer between the gas bulk and the liquid bulk: the first one being the transfer of the gas from the bulk to the gas-liquid interphase, then the interphase itself, and finally from the liquid interphase to the liquid bulk (Doran, 1995).

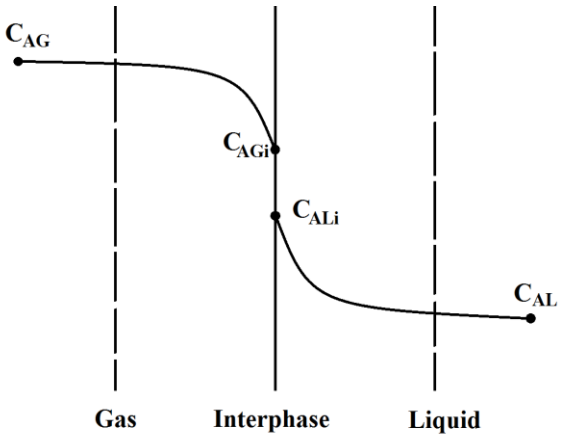

Figure 1. Diagram of the gas-liquid interface, with their respective concentrations. C_{AG}, concentration of the compound A in the gas phase bulk; C_{AL}, concentration of A in the liquid phase bulk; C_{AG_i} and C_{AL_i}, concentration of A in the gas and liquid interphase, respectively.

The liquid-phase mass transfer dominates the overall phenomena when working with gases with low solubility (like oxygen or hydrogen). The concentration at the liquid interphase can

be considered equal to the liquid concentration in equilibrium with the gas concentration in the bulk.

$$N_A = k_L a \cdot (C_{AL}{}^* - C_{AL}) \quad (1)$$

where N_A is the rate of mass transfer of component A through the gas-liquid interphase, $k_L a$ is the combined mass-transfer coefficient, $C_{AL}{}^*$ is the concentrations of A in the liquid phase in equilibrium with C_{AG}, and C_{AL} is the actual concentration in the liquid phase. It can be noticed that the driven force for the mass transfer is the difference between the equilibrium and the current concentration. In some cases, these values can be directly measured. If it is not possible, they can be smoothly calculated. Nevertheless, the mass-transfer coefficient is not easy to estimate due to the nature of the fluids and the experimental conditions. The composition of the liquid and gas phases, the stirring conditions, the geometry of the fluids container, and many other factors affect this coefficient. Most authors have proposed models with the following structure (Cooper et al., 1944; H Fukuda et al., 1968 (a); H. Fukuda et al., 1968 (b); Richards, 1961; Van'T Riet, 1979)

$$k_L a = K \cdot \left(\frac{P}{V}\right)^{\alpha} \cdot (v_s)^{\beta} \cdot N^{\gamma} \quad (2)$$

where K, α, β and γ are constants that depend on the operating conditions as well as the geometry of the reactor, while P/V, v_s and N are the volumetric power, the superficial gas velocity, and frequency of the rotation of the mixer, respectively. As can be presumed, using Equation 2 outside the boundaries of confidence will give inaccurate values. Besides, these equations were proposed for oxygen transfer, which obligates the researcher to use the diffusivity correlation between the gases and estimate the $k_L a$ of the scoped gas (Kery et al., 2019). Another option for calculating the $k_L a$ is using dynamic methods (Munasinghe and

Khanal, 2010), which take much time and resources and also require an online measure of the dissolved gas, which sometimes, as described before, is not available.

This work presents a feasible method to estimate the time needed to remove a gaseous component from a liquid medium by replacing it with another gas (gas changing time). It is estimated using a classical and simplified liquid-gas phase equilibrium model. In particular, this work aims to describe a method that can be easily applied in the laboratory. It considers actual operational conditions and requires a few analytical instruments (i.e. gas analyzer) and informatics tools (i.e. an informatics program able to manage spreadsheets).

2. Materials and methods

2.1 Liquid phase composition

The liquid phase used in gas changing experiments was a culture medium for anaerobic bacteria. In 1 L of water, the medium contained K_2HPO_4 8.44 g; NaCl 2.9 g; yeast extract 2 g; KH_2PO_4 1.76 g; NH_4Cl 1 g; cysteine hydrochloride 0.5 g; $MgSO_4$ 0.180 g; resazurin 1 mg. Chemical reagents were purchased from Merck (DE).

2.2 Bioreactors

The reactor used for N_2 to CO_2 gas change and *vice versa* was a custom-adapted bioreactor manufactured by the H.E.L group (UK). The system consisted of a 2 L oil-jacketed vessel, 5 piston pumps for liquid injection (culture broth, base, acid, trace elements, and anti-foam), 4 Mass Flow Controller (MFC) for high in-flow gas rates (H_2, CO_2, N_2, CO) (Vögtlin Instruments, CH) and 2 low in-flow gas rates MFCs (CO_2 and H_2) (Bronkhorst High-Tech BV, NL). Sparging of the gas was applied from the bottom of the vessel (via a micrometric

sparger). Stirring of the medium was mechanically maintained by one level of Ruston blades connected to an impeller driven by a motor and baffles. An oil bath connected to the jacket of the reactor allowed for sterilization (autoclaving of the vessel) and maintained the operating temperature during experiments. The head plate of the reactor vessel was fitted with pH, redox, liquid level, pressure, and temperature probes. A Back Pressure Regulation (BPR) valve allowed pressure control at defined setpoints. The vessel was filled with 1L of sterile medium during the gas changing experiments. The in-flow gas rate applied was 4.5 L/h, the stirring 400 rpm, and the reactor temperature 30°C.

The gas from the reactor outlet was released in a chemical hood or collected in sample bags and analyzed by an off-line micro-GC. In experiments from N_2 to CO_2, the liquid medium pumped in the reactor was previously sparged with 100% N_2 to remove oxygen. Gas out sampling started immediately after the activation of the MFC for CO_2.

The reactor used for the gas change from air to N_2 and *vice versa* was a Biostat A reactor (Sartorius Stedim Biotech, DE) consisting of a glass vessel of 1.5 L total volume, 4 peristaltic pumps for liquid injection (culture broth, base, acid, and anti-foam), 2 MFCs (Air and N_2). Stirring of the medium was mechanically provided by two levels of Rushton blades. The reactor was sterilized by autoclaving. An electric heater placed around the outer side of the glass vessel maintained a constant temperature during experiments. The head plate of the reactor vessel was fitted with pH, foam, and temperature probes. During the gas changing experiments, the vessel was filled with 0.5 L of sterile medium. The in-flow rate applied was 6 L/h, the stirring was 100 rpm, and the temperature was 30°C. The gas out from the reactor was directly analyzed by a micro-GC. In the experiment from air to N_2, the liquid medium was pumped into the reactor without oxygen purging. Gas out sampling started when MFC for 100% N_2 was switched on.

2.3 Analytics and software

Gas composition for in-flowing and out-flowing gas was measured using an Agilent 490 Micro GC (Agilent, CA, USA) or a Micro GC Fusion (Inficon, CH). Agilent 490 Micro GC is equipped with the analytical columns Molsieve 5Å, using Argon as the carrier, and PoraPLOT U using Helium as the carrier. Micro GC Fusion is equipped with the analytical columns Molsieve 5Å and Rt-U-Bond, using Argon and Helium as carriers, respectively. Excel 2016 32-bit (Microsoft, USA) was used to analyze the experimental data to estimate the gas changing time.

2.4 Statistics

Two statistic indicators were calculated to evaluate how the predictive model and the real data correlated: the coefficient of determination (R^2) and the standard error of the estimate (σ_{est}), (Eq. (3) and (4) respectively). The statistical analysis was performed on the logarithmic results.

$$R^2 = 1 - \frac{\sum_{i=1}^{n}(y_i - y_i')^2}{\sum_{i=1}^{n}(y_i - \bar{y})^2} \quad (3)$$

$$\sigma_{est} = \sqrt{\frac{\sum_{i=1}^{n}(y_i - y_i')^2}{n}} \quad (4)$$

where:

y_i: is an actual experimental value.

y_i': is the predicted value.

n: is the number of experimental data.

$\bar{y}$: is the mean value of the experimental data.

Formatted: Not Highlight
Formatted: Not Highlight
Formatted: Not Highlight
Formatted: Not Highlight
Formatted: Not Highlight
Formatted: Not Highlight
Formatted: Not Highlight
Formatted: Not Highlight
Formatted: Not Highlight
Formatted: Not Highlight
Formatted: Not Highlight
Formatted: Not Highlight
Formatted: Not Highlight
Formatted: Not Highlight
Formatted: Not Highlight
Formatted: Not Highlight
Formatted: Not Highlight
Formatted: Not Highlight
Formatted: Not Highlight
Formatted: Not Highlight

3. Results

3.1 Model

The model formulated was based on the following system (Figure 2). A certain gas (*i*) is bubbled at a rate of $G_{in} \cdot y_{i,in}$ in a reactor with V_L volume of liquid and V_G volume of gas in the headspace. The temperature (T) and the pressure (P) is fixed. The gas outlet (G_{out}) has a fraction of the i gas ($y_{i,out}$). Inside the liquid phase, there is a certain concentration of dissolved gas ($C_{i,L}$).

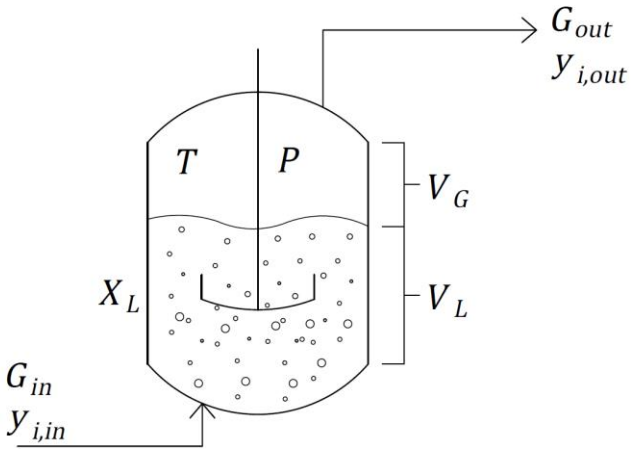

Figure 2. The system considered in the model.

Where:

G: Molar Flow (mmol/min).

y: Molar fraction in the gas.

184 V: Volume (m^3).

185 C: Concentration ($mmol/m^3$).

186 T: Temperature (K).

187 P: Pressure (Pa).

188 Subscript:

189 L: in/of the liquid.

190 G: in/of the gas.

191 in: Inlet.

192 out: Outlet.

193 *i*: from compound *i*.

194 Three mass balances can be proposed for this system: the global balance of compound *i* (Eq.
195 5), the balance of compound *i* in the liquid phase (Eq. 6), and the balance of compound *i* in
196 the gas phase (Eq. 7) which assumes the gas as an ideal one.

$$\frac{dn_i}{dt} = G_{in} \cdot y_{i,in} - G_{out} \cdot y_{i,out} \quad (5)$$

$$\frac{dn_{i,L}}{dt} = k_L a \cdot V_L \cdot \left(C^*_{i,L} - C_{i,L}\right) \quad (6)$$

$$\frac{dn_{i,G}}{dt} = \frac{V_G}{R \cdot T} \cdot \frac{dp_i}{dt} \quad (7)$$

197 where n_i are the moles of the *i* compound, p_i is the partial pressure of *i* in the headspace, and
198 $C^*_{i,L}$ is the equilibrium concentration of *i* in the liquid.

199 The global accumulation of moles in the system will be equal to the sum of the accumulation
200 in both gas and liquid phases (Eq. 8).

201

$$\frac{dn_i}{dt} = \frac{dn_{i,L}}{dt} + \frac{dn_{i,G}}{dt} \tag{8}$$

202

203 This allows the generation of a new equation (Eq. 9) by replacing Eq (5), (6), and (7) in (8).

$$\frac{V_G}{R \cdot T} \cdot \frac{dp_i}{dt} = G_{in} \cdot y_{i,in} - G_{out} \cdot y_{i,out} - k_L a \cdot V_L \cdot \left(C^*_{i,L} - C_{i,L}\right) \tag{9}$$

204 On the other hand, from Eq (6), it is possible to obtain a relation between time and $C_{i,L}$

205 (assuming $C^*_{i,L}$ constant during short periods).

$$V_L \cdot \frac{dC_{i,L}}{k_L a \cdot V_L \cdot \left(C^*_{i,L} - C_{i,L}\right)} = dt \tag{10}$$

$$\int \frac{dC_{i,L}}{k_L a \cdot \left(C^*_{i,L} - C_{i,L}\right)} = \int dt \tag{11}$$

$$\frac{-1}{k_L a} \cdot \left(\ln\left(C^*_{i,L} - C_{i,L}\right) - \ln K\right) = t \tag{12}$$

$$\ln \frac{\left(C^*_{i,L} - C_{i,L}\right)}{K} = -t \cdot k_L \mathrm{a} \tag{13}$$

$$\frac{\left(C^*_{i,L} - C_{i,L}\right)}{K} = e^{-t \cdot k_L \mathrm{a}} \tag{14}$$

$$C_{i,L} = C^*_{i,L} - K \cdot e^{-t \cdot k_L a} \tag{15}$$

206 where K is the constant of integration. By replacing Eq. (15) into Eq. (9) the following

207 expression is obtained

$$\frac{V_G}{R \cdot T} \cdot \frac{dp_i}{dt} = G_{in} \cdot y_{i,in} - G_{out} \cdot y_{i,out} - k_L a \cdot V_L \cdot \left(C^*_{i,L} - C^*_{i,L} + K \cdot e^{-t \cdot k_L a}\right) \quad (16)$$

If no *i* compound is injected into the system ($y_{i,in} = 0$), Eq. (16) could be expressed as

$$\frac{V_G}{R \cdot T} \cdot \frac{dp_i}{dt} + G_{out} \cdot y_{i,out} = -k_L a \cdot V_L \cdot K \cdot e^{-t \cdot k_L a} \quad (17)$$

Since the partial pressure of the *i* compound (p_i) in the headspace will be equal to the total pressure (P) times the molar fraction in the outlet stream, Eq. (17) becomes:

$$\frac{V_G}{R \cdot T} \cdot \frac{d\left(P \cdot y_{i,out}\right)}{dt} + G_{out} \cdot y_{i,out} = -k_L a \cdot V_L \cdot K \cdot e^{-t \cdot k_L a} \quad (18)$$

Assuming a constant pressure during the whole process, Eq. (18) can be rewritten as

$$\frac{V_G \cdot P}{R \cdot T} \cdot \frac{dy_{i,out}}{dt} + G_{out} \cdot y_{i,out} = -k_L a \cdot V_L \cdot K \cdot e^{-t \cdot k_L a} \quad (19)$$

Besides, we can assume that:

$$\frac{V_G \cdot P}{R \cdot T} = n_G \quad (20)$$

$$n_G \cdot \frac{dy_{i,out}}{dt} + G_{out} \cdot y_{i,out} + k_L a \cdot V_L \cdot K \cdot e^{-t \cdot k_L a} = 0 \quad (21)$$

where n_G is the total amount of gas moles in the system. By solving the differential equation, Eq. (22) is obtained:

$$y_{i,out} = K_1 \cdot e^{-t \cdot \frac{G_{out}}{n_G}} + \frac{k_L a \cdot V_L \cdot K \cdot e^{-t \cdot k_L a}}{k_L a \cdot n_G - G_{out}} \tag{22}$$

where K_1 is a new constant that comes from the solution of the differential equation. In Eq. (22), it can be noticed that if $G_{out} \ll k_L a \cdot n_G$ then

$$y_{i,out} \approx K_1 \cdot e^{-t \cdot \frac{G_{out}}{n_G}} + \frac{V_L \cdot K}{n_G} \cdot e^{-t \cdot k_L a} \tag{23}$$

Since the value of the first exponent will be greater than the second and if the constants have the same order of magnitude, the first term will dominate the value of $y_{i,out}$.

$$y_{i,out} \approx K_1 \cdot e^{-t \cdot \frac{G_{out}}{n_G}} \tag{24}$$

On the other side, if $G_{out} \gg k_L a \cdot n_G$ then

$$y_{i,out} \approx K_1 \cdot e^{-t \cdot \frac{G_{out}}{n_G}} - \frac{k_L a \cdot V_L \cdot K}{G_{out}} \cdot e^{-t \cdot k_L a} \tag{25}$$

At the beginning of the gas change process, the value of $\frac{k_L a \cdot V_L \cdot K}{G_{out}}$ in Eq. (25) makes the second term have a small influence on the value of $y_{i,out}$. As time passes, the rate of decrease is greater. Nevertheless, since $y_{i,out}$ cannot take negative values, the value of the second term cannot be greater than the first one. Hence, for small values of time:

$$y_{i,out} \approx K_1 \cdot e^{-t \cdot \frac{G_{out}}{n_G}} \tag{26}$$

It can be noticed that the two variables that can be controlled by changing the stirring speed or the gas flow ($k_L a$ and G_{out}) can dominate the process. When the molar flow dominates the process ($G_{out} \gg k_L a \cdot n_G$), the phenomenon occurs faster rather than when the volumetric gas transfer coefficient ($G_{out} \ll k_L a \cdot n_G$) dominates the process. Besides, since $k_L a$ depends on the volumetric power that is controlled by the stirring rate and the flow, the relation between G_{out} and $k_L a$ can be described as a relation between G and the stirring velocity of the reactor. This could be researched in future work.

This simplified exponential model will describe the decay of the concentration of a purged gas and it can be applied to predict the gas exchange time of a determined system if the constant parameters are available. Using a semilogarithmic graph the slope will represent the value of $\frac{G_{out}}{n_G}$ and the intercept the logarithm of K_1. The following section describes the protocol to obtain the gas change time.

3.2. Protocol

To estimate the gas changing time the following steps need to be executed:

1) Take a sample of the outlet flow of gas from the reactor at the beginning of the gas changing process and measure its molar composition in percentage or fraction through a gas analyzer.
2) Repeat the same process regularly with an interval of time determined by the researcher. An interval of 5 minutes is recommended .
3) The sampling can stop after the fraction of the purged gas reaches half of its value at the beginning of the gas changing process.
4) On a spreadsheet, create a graph with the time values on the X-axis and the natural logarithm of the fraction or percentage of the purged gas on the Y-axis.
5) Obtain the linear regression of the data.
6) Obtain the equation of the linear regression line and the R-squared value.
7) The R-squared value needs to be higher than 0.99.
8) Graphically obtain the value of time that will fulfill the desired gas change. The linear regression intercept will be approximately $\ln(K_1)$ and the slope $-\frac{G_{out}}{n_G}$ of Eq. (22).

3.3. Model validation

Figures 3-6 report the decrease of the gas purged from the reactor throughout the gas changing experiments. Figures 3 and 4 show data from N_2 to CO_2 and from CO_2 to N_2, respectively. Similarly, Figures 5 and 6 describe experiments using air and N_2. According to the analysis of the in-let gas, air sparged in the reactor had 20.9 % of O_2 and 79.05% of N_2. The purge of air using pure nitrogen and *vice-versa* was evaluated by monitoring the variation of the oxygen molar fraction in the out-gas.

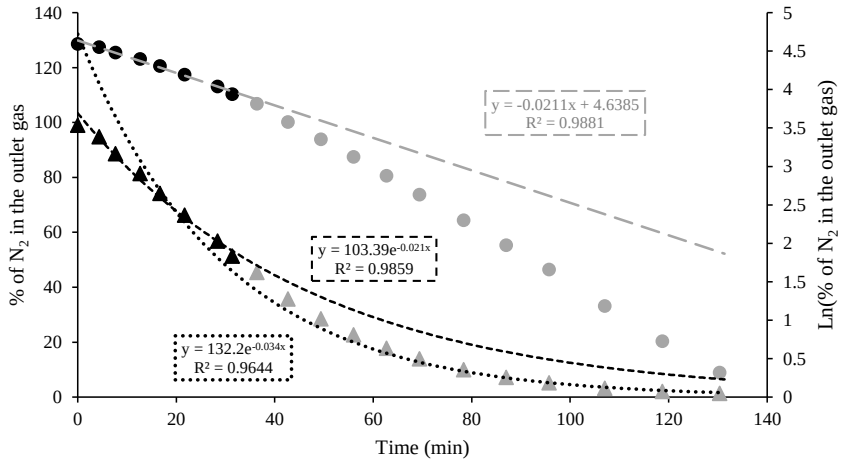

Figure 3: Purging of nitrogen using carbon dioxide. Triangles: experimental values; Dots: natural logarithm of the experimental data; Dotted black line: exponential curve generated by all the experimental data; Dashed black line: exponential curve obtained by using black triangles; Dashed gray line: linear curve obtained by considering the black dots.

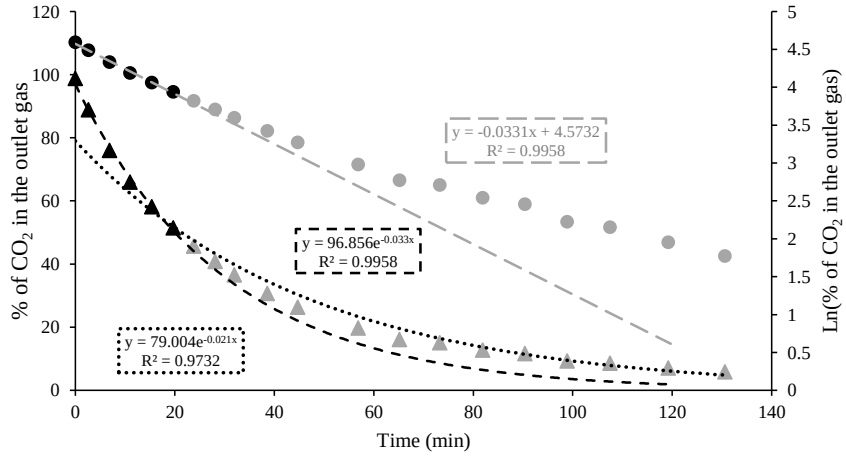

Figure 4: Purging of carbon dioxide using nitrogen. Triangles: experimental values; Dots: natural logarithm of the experimental data; Dotted black line: exponential curve generated by all the experimental data; Dashed black line: exponential curve obtained by using black triangles; Dashed gray line: linear curve obtained by considering the black dots.

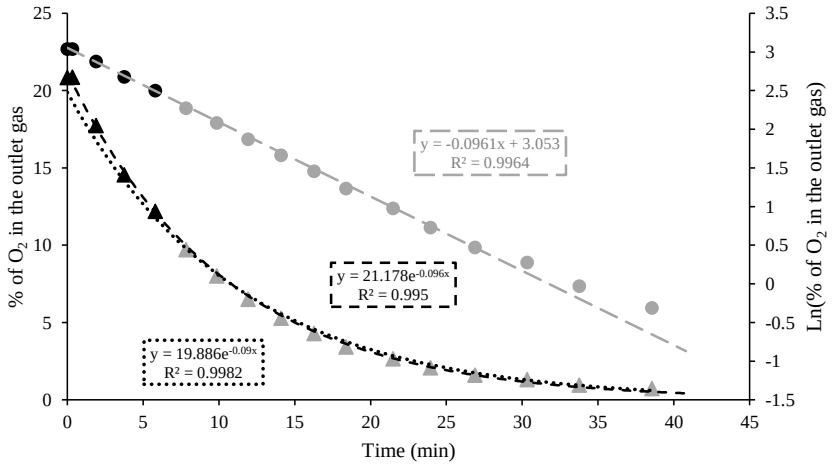

Figure 5: Purging of air using nitrogen. Triangles: experimental values; Dots: natural logarithm of the experimental data; Dotted black line: exponential curve generated by all the experimental data; Dashed black line: exponential curve obtained by using black triangles; Dashed gray line: linear curve obtained by considering the black dots.

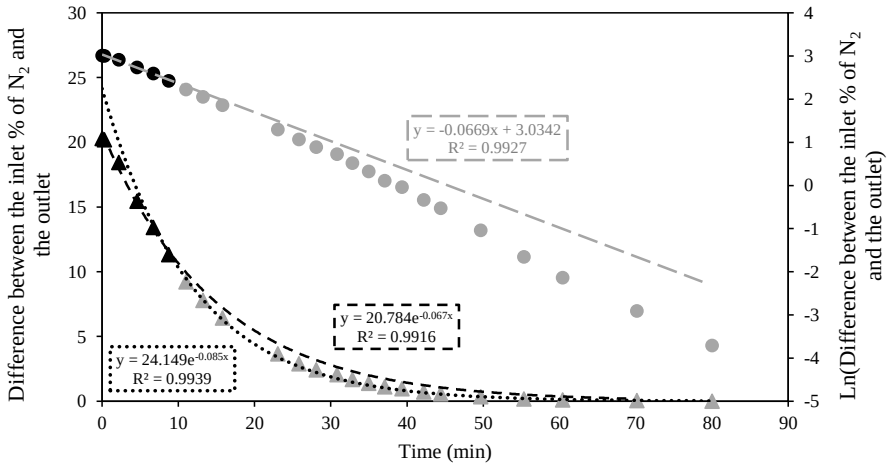

Figure 6: Purging of nitrogen using air. Triangles: experimental values; Dots: natural logarithm of the experimental data; Dotted black line: exponential curve generated by all the experimental data; Dashed black line: exponential curve obtained by using black triangles; Dashed gray line: linear curve obtained by considering the black dots.

Experimental data were plotted and the model was applied. The correlation between data and the model was evaluated. It can be seen that data from each experiment fit an exponential curve (dotted black lines in Figures 3-6). Following the protocol, the linear correlation between the natural logarithm of the out-gas composition and the time was obtained for each purged gas (black dots and dashed gray line in Figures 3-6). It can be seen that in experiments involving carbon dioxide the predicting lines did not correlate accurately with the experimental data, whereas in the experiments with air and nitrogen the predictive models fit the experimental data with greater precision. Table 1 reports the statistics calculated for each gas changing experiment.

Formatted: Not Highlight

Table 1: Statistical analysis between the predictive model and the experimental data.

Experiment	N_2 to CO_2	CO_2 to N_2	Air to N_2	N_2 to air
n	20	15	17	24
$\sum_{i=1}^{n}(y_i - y_i')^2$	8.57	7.98	0.17	7.82
$\sum_{i=1}^{n}(y_i - \bar{y})^2$	34.24	15.06	19.12	84.88
R^2	0.7496	0.47	0.9909	0.9079
σ_{est}	0.6547	0.6318	0.101	0.5707

The value of the X-axis maked it possible to extract the time that fulfills the desired gas change. For example, in the experimental condition applied, complete purging of oxygen using nitrogen required around 40 minutes (Figure 5). The maximum difference between the modeled values and experimental data was 0.4%. For the experiments involving CO_2, a different reactor was used and other experimental conditions were applied. Therefore, a different gas changing time was needed. Figure 3 shows that the time required to completely change the gas from nitrogen to carbon dioxide was around 200 minutes. The error between the model and the experimental data was more variable. In fact, when the gas change was completed, the error was 1.9 % of the gas composition. In the central part of the curve, at around 70 minutes, the maximum error was of 9.9 %.

4. Discussion

The protocol proposed describes an easily applicable method to estimate the gas changing time in the laboratory routine. It aims to consume little time and resources, considering actual operating conditions, and requires few analytic instruments and informatics tools.

In all the experiments, the error between the actual values and the values predicted by the model was less than 10% of the gas composition. The biggest difference recorded was in

experiments involving CO_2. In experiments that did not involve carbon dioxide, the maximum error was reduced to less than 0.8%. The bigger error found with CO_2 could be explained by the chemical equilibrium that carbon dioxide has in aqueous solutions, which is not considered in the proposed model. In fact, carbon dioxide reacts with water and produces carbonic acid. This reaction has slow kinetics (for more details see Stumm and Morgan, 1995) and creates a stock of CO_2 in the liquid phase, which moves towards equilibrium with the gas phase. It can explain why the predictive model showed a faster decrease in the CO_2 fraction than the measured values (Figure 4). Another factor that could have affected results with CO_2 was the variable pressure inside the reactor during the gas change. In the experiments that involved this gas, the pressure fluctuated between 1.51 bar and 1.76 bar. In particular, the reactor pressure was set at 1.76 bar, with a constant in-flow gas rate and opening of the valve for pressure regulation. After starting the sparging of the medium with CO_2, the pressure quickly decreased to 1.51 bar. It then returned to the initial value (1.76 bar) when the gas change was completed. The assumption of a constant pressure done during the deduction of the model might explain the discrepancy between the experimental data and the model.

According to the statistical analysis, the air to N_2 model best correlated to the experimental data, followed by the N_2 to air change. When the gas change was from nitrogen to carbon dioxide, the coefficient of determination was higher than when it was from carbon dioxide to nitrogen. Considering the value of the standard error of the estimate, the accuracy of the gas change from carbon dioxide to nitrogen is slightly more accurate than the reverse process experiment. Nevertheless, in both cases, the statistical analysis suggested a worse accuracy of the model in experiments involving CO_2 than in experiments involving air, probably due to the effect of the chemical equilibrium of carbon dioxide in water.

Formatted: Not Highlight

The model is for researchers looking for an affordable and practical method to improve their experiments' efficiency. The specific experimental conditions and the constraints related to the availability of analytical instruments can make the time between each measurement very variable. This work found out that, purging oxygen, the model could fit very well with the experimental data measuring only two samples, one at the beginning and another when the gas was half of its initial concentration (Figure 7).

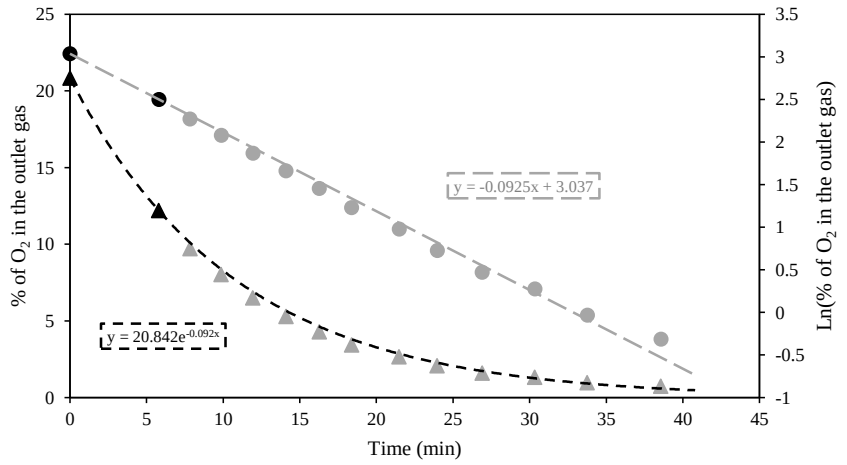

Figure 7: Purging of air using nitrogen. Triangles: experimental values; Dots: natural logarithm of the experimental data; Dashed black line: exponential curve obtained by using only black triangles; Dashed gray line: linear curve obtained by considering the black dots.

It is important to remember that the time required for gas change inside the reactor will vary with the conditions of stirring, temperature, pressure, gas in-flow rate, gas and media compositions. If the conditions do not change, the time predicted in one experiment can be

used in the following experiments. If one or more factors change, it is recommended to re-evaluate the gas changing time using this protocol.

5. Conclusion

The proposed protocol allows researchers to predict the time required to completely exchange the gas in a reactor containing liquid media, and it takes into account the actual experimental condition applied in a specific run. Purging of an unwanted gas from the reactor often is based on bibliographic data. These calculations, in many cases, are not accurate enough for a specific situation because of the differences in both reactor and experimental settings (reactor design, working volume of liquid and gas phases, in-flow rate of a specific gas, stirring equipment and speed). The described protocol can be easily implemented in the laboratory. Hence, it seeks to be simple for sampling procedure, calculation, and requirements in terms of human and time efforts, equipment, and software.

The model's correlation and accuracy were high when air was purged with nitrogen, which is often the first step in setting up an anaerobic fermentation. For cases involving CO_2, the correlation and the accuracy were lower. To improve the model, specific CO_2 modeling should include the chemical equilibrium of this gas in water. Moreover, a comparison between the k_La-dominant process and the molar flow-dominant process should also be performed for further model validation. Nevertheless, the proposed methodology for calculating the gas changing time will contribute to the efficient use of resources and time during experiments involving other gases, mainly oxygen, which is a pivotal step for many processes involving anaerobic reactions.

Formatted: Not Highlight

Acknowledgments

We would like to thank Prof. Germán Eduardo Aroca Arcaya, Prof. Raúl Conejeros (Pontificia Universidad Católica de Valparaíso, Valparaíso, Chile) and Giuseppe Pietricola, Ph.D. (Politecnico di Torino, Torino, Italy) for advices and revisions that improved the manuscript. Moreover, we would like to thank Prof. Carminna Ottone (Pontificia Universidad Católica de Valparaíso, Valparaíso, Chile) for supporting the mobility between the research institutions allowing this collaboration.

Fundings

This research did not receive any specific grant from funding agencies in the public, commercial, or not-for-profit sectors.

References

Al Rowaihi, I.S., Kick, B., Grötzinger, S.W., Burger, C., Karan, R., Weuster-Botz, D., Eppinger, J., Arold, S.T., 2018. A two-stage biological gas to liquid transfer process to convert carbon dioxide into bioplastic. Bioresour. Technol. Reports 1, 61–68. https://doi.org/10.1016/j.biteb.2018.02.007

Chauvy, R., Meunier, N., Thomas, D., De Weireld, G., 2019. Selecting emerging CO2 utilization products for short- to mid-term deployment. Appl. Energy 236, 662–680. https://doi.org/10.1016/j.apenergy.2018.11.096

Cooper, C.M., Fernstrom, G.A., Miller, S.A., 1944. Performance of Agitated Gas-Liquid Contactors—Correction, Industrial and Engineering Chemistry. UTC.

https://doi.org/10.1021/ie50417a601

Doran, P.M., 1995. Bioprocess Engineering Principles. Academic press.

Fukuda, H., Sumino, Y., Kansaki, T., 1968. Modified equations for volumentric oxygen transfer coefficient. J. Ferment. Technol. 46, 829–837.

Fukuda, H, Sumino, Y., Kanzaki, T., 1968. Scale-Up of Fermenters. II. Modified Equations for Power Requirement. J. Ferment. Technol. 46, 838.

Hoffmeister, S., Gerdom, M., Bengelsdorf, F.R., Linder, S., Flüchter, S., Öztürk, H., Blümke, W., May, A., Fischer, R.J., Bahl, H., Dürre, P., 2016. Acetone production with metabolically engineered strains of Acetobacterium woodii. Metab. Eng. 36, 37–47. https://doi.org/10.1016/j.ymben.2016.03.001

Kantzow, C., Weuster-Botz, D., 2016. Effects of hydrogen partial pressure on autotrophic growth and product formation of Acetobacterium woodii. Bioprocess Biosyst. Eng. 39, 1325–1330. https://doi.org/10.1007/s00449-016-1600-2

Kery, K., Kresnowati, P., Setiadi, T., 2019. Evaluation of gas mass transfer in reactor for syngas fermentation. AIP Conf. Proc. 2085. https://doi.org/10.1063/1.5094986

Maddipati, P., Atiyeh, H.K., Bellmer, D.D., Huhnke, R.L., 2011. Ethanol production from syngas by Clostridium strain P11 using corn steep liquor as a nutrient replacement to yeast extract. Bioresour. Technol. 102, 6494–6501. https://doi.org/10.1016/j.biortech.2011.03.047

Munasinghe, P.C., Khanal, S.K., 2010. Syngas fermentation to biofuel: Evaluation of carbon monoxide mass transfer coefficient (kLa) in different reactor configurations. Biocatal. Bioreact. Des. 26, 1616–1621. https://doi.org/10.1002/btpr.473

Richards, J.W., 1961. Studies in aeration and agitation. Prog Ind Microbiol 3, 141–172.

Saravanan, A., Senthil kumar, P., Vo, D.V.N., Jeevanantham, S., Bhuvaneswari, V., Anantha

Narayanan, V., Yaashikaa, P.R., Swetha, S., Reshma, B., 2021. A comprehensive review on different approaches for CO2 utilization and conversion pathways. Chem. Eng. Sci. 236, 116515. https://doi.org/10.1016/j.ces.2021.116515

Shi, J., Jiang, Y., Jiang, Z., Wang, Xueyan, Wang, Xiaoli, Zhang, S., Han, P., Yang, C., 2015. Enzymatic conversion of carbon dioxide. Chem. Soc. Rev. 44, 5981–6000. https://doi.org/10.1039/c5cs00182j

Straub, M., Demler, M., Weuster-Botz, D., Dürre, P., 2014. Selective enhancement of autotrophic acetate production with genetically modified Acetobacterium woodii. J. Biotechnol. 178, 67–72. https://doi.org/10.1016/j.jbiotec.2014.03.005

Stumm, W., Morgan, J.J., 1995. Aquatic chemistry : Chemical equilibria and rates in natural waters, John Wiley & Sons. https://doi.org/10.1094/asbcmoa-beer-13

Van'T Riet, K., 1979. Review of Measuring Methods and Results in Nonviscous Gas-Liquid Mass Transfer in Stirred Vessels. Ind. Eng. Chem. Process Des. Dev. 18, 357–364. https://doi.org/10.1021/i260071a001